



Title	Diffusion Welding of Molybdenum to Hastelloy Alloy X
Author(s)	Enjyo, Toshio; Oouchi, Mitsuo; Nasu, Saburo et al.
Citation	Transactions of JWRI. 1977, 6(1), p. 131-137
Version Type	VoR
URL	<a href="https://doi.org/10.18910/12548">https://doi.org/10.18910/12548</a>
rights	
Note	

*The University of Osaka Institutional Knowledge Archive : OUKA*

<https://ir.library.osaka-u.ac.jp/>

The University of Osaka

# Diffusion Welding of Molybdenum to Hastelloy Alloy X†

Toshio ENJYO\*, Mitsuo OOUCHI\*\*, Saburo NASU\*\*\*, Kenji IKEUCHI\*\*\*  
and Yoshiaki ARATA\*

## Abstract

Diffusion welding between pure molybdenum and heat-resisting alloy Hastelloy X has been performed in vacuum at the temperature range of 750°C–1200°C. Two steps welding technique including a short time annealing at high temperature (1 minute at 1200°C) increases the real metal-contact between molybdenum and Hastelloy alloy X, and takes the improvements in joint strength. Furthermore, this technique is useful not to enlarge the deformation at weld joint. Application of Ni insert-metal suppresses the formation of brittle intermetallic compound, P phase, and increases the joint strength. However, the formation of binary compound,  $\delta$ -MoNi, was observed at bonding interface. Fracture of the weld joints by the tensile strength tests at room temperature has occurred always through the intermetallic compounds and also along the grain boundaries of molybdenum base metal. After the welding procedure, the voids and MoO<sub>2</sub> were found out at the grain boundaries of molybdenum using scanning electron microscopy (SEM) and transmission electron microscopy (TEM) techniques.

## 1. Introduction

It is well known that molybdenum will be used in structure components of nuclear reactor, especially for the blanket structure components in future fusion reactor, since the molybdenum is one of the refractory metals and has some good characteristic properties at high temperatures<sup>1)</sup>. Heat-resisting alloy Hastelloy X will be used also as components of coolant and heat-converter in high temperature gas fission reactor. If good weld joints are easily obtained between molybdenum and Hastelloy alloy X, the construction of new heat-converter using these materials will become to be good situation in its design. However, it is quite difficult by usual fusion welding technique to get a good weld joints between dissimilar metals and alloys. Diffusion welding technique which is a typical method in solid state bonding has to apply to get a good weld joints in these dissimilar metals and alloys<sup>2,3,4)</sup>.

In this investigation the first attempt has been performed to get the weld joints between molybdenum and Hastelloy alloy X utilizing the diffusion welding

technique. Tensile strength at room temperature obtained from the weld joint is discussed in terms of the effects of methods in welding procedure and a use of Ni insert-metal. Two steps welding technique is appreciable to improve the tensile strength of weld joints without the increase of the percent reduction in length. Ni insert-metal suppresses the formation of brittle intermetallic compound and increases the magnitude of the tensile strength. Microscopic observations about fractured surface were performed and the existence of voids was found out along grain boundaries in molybdenum. Metallographical results obtained were discussed in final sections.

## 2. Experimental Details.

### 2.1. Specimen.

Chemical compositions of material used in this investigation are listed in **Table 1**. Rod shaped specimens were 30 mm in length and 20 mm in diameter. Surface of the specimen was machined by lathe and degreased by acetone just before welding procedures.

Table 1 Chemical Compositions (wt. %).

	C	Mn	Si	P	S	Cr	Mo	W	Fe	B	Ni	Co	Al	Ti
Hastelloy X	0.08	0.63	0.03	<0.005	<0.005	21.98	8.81	0.54	18.35	0.001	Bal.	Tr.	Tr.	0.02
Molybdenum							99.97		0.004					

† Received on April 8, 1977 (Submitted originally in J. Japan Weld. Soc., (1977), in Japanese.)

\* Professor

\*\* Japan Atomic Energy Research Institute of Tokai Establishment

\*\*\* Research Instructor

Surface roughness was estimated to be 3-S in JIS standard number. Table 2 shows the micro-Vicker's hardness number and grain size for the specimens. Grain of molybdenum elongated toward the direction in length. Ni thin foils, about  $10\ \mu$  in thickness, were used as insert-metals.

Table 2 Vicker's Hardness Number and Grain Size for as received Materials.

	Vicker's Hardness Number ( $H_V$ ).	Grain Size ( $\mu$ )
Hastelloy Alloy X	170	43
Molybdenum	220	190* 40**

\* estimated from longitudinal cross section of the specimen.

\*\* estimated from transverse cross section of the specimen.

## 2.2. Welding conditions and methods in metallography.

Normal diffusion welding and two steps diffusion welding procedures as shown in Fig. 1 were applied in this experiment. Welding parameters in Fig. 1 are as follows; externally applied pressure is constant, temperature  $T_1$  is  $1200^\circ\text{C}$ ,  $T_0$  is temperature ranged from  $750^\circ\text{C}$  to  $1200^\circ\text{C}$ , time  $t_1$  is 1 minute and time  $t_0$  is 30 minutes, respectively. Apparatus for diffusion welding was reported previously<sup>4)</sup> and the method to measure the temperature at weld interface was also described in previous paper<sup>4)</sup>. Welding was performed under the condition of vacuum at about  $1 \times 10^{-4}$  Torr. Instron type machine was used for the tensile strength measurements. Its gauge length was 30 mm and the strain rate was constant at  $5.6 \times 10^{-4}$ /sec. The following metallographical observations were performed in order to clarify the microstructure near weld bond region and the effects of Ni insert-metal. Using optical and scanning electron microscopies, the fractured surfaces at weld bond region were observed. Scanning electron microscopy (SEM) was Hitachi type HSM-2B and its operation was performed at acceleration voltage of 20 kV. Distribution of the elements was also estimated by scanning analysis of characteristic X-rays using a Si(Li) solid state detector (SSD) combined in SEM. Both side of the fractured surfaces were analysed by the X-ray diffraction technique in order to identify the intermetallic compounds formed at weld bond region. Microstructure of molybdenum near the weld bond region was observed by transmission electron micro-

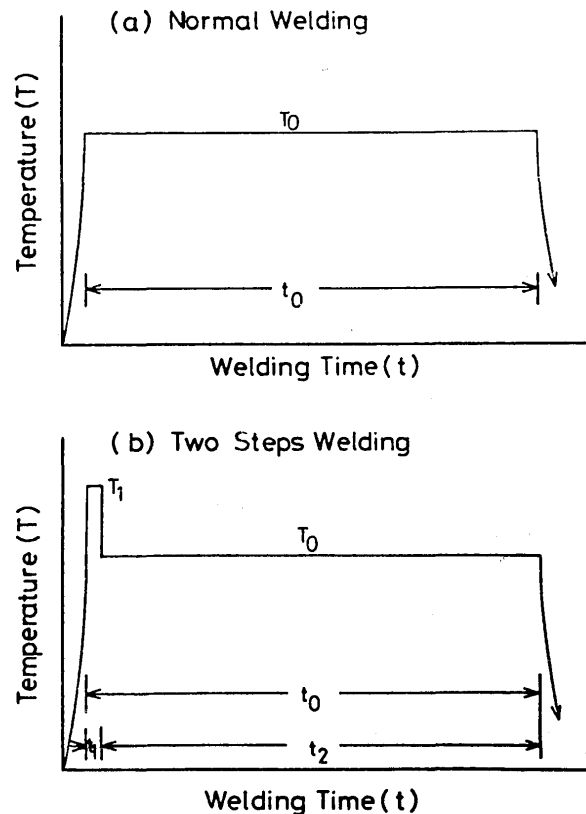


Fig. 1 Schematic diagrams for experimental diffusion welding procedures. (a) Normal welding, that is one step diffusion welding. (b) Two steps diffusion welding. Welding conditions are as follows;  $t_0=30$  minutes,  $t_1=1$  minute,  $T_1=1200^\circ\text{C}$  and  $T_0=\text{variable}$ .

scopy (TEM) after the thinning procedures of specimen, using Hitachi type HU-12A electron microscopy whose acceleration voltage was always 125 KV.

## 3. Experimental Results and Discussions.

### 3.1. Two steps diffusion welding.

Tensile strength and percent reduction in length obtained from normal diffusion welding for 30 minutes at  $950^\circ\text{C}$  are shown in Fig. 2 as a function of externally applied pressure. Increasing the pressure, the magnitude of the tensile strength increases and the large magnitude of pressure may be necessary to get higher strength in weld joints. This result shows the tensile strength of the weld joint largely depends on the behavior at initial stage of welding process in which the true metal-contact at the weld interface are induced by the deformation of micro-asperities at surfaces. High pressure and high temperature are necessary for accomplishment in diffusion welding between molybdenum and Hastelloy alloy X, since both materials are heat-resisting materials and have a high

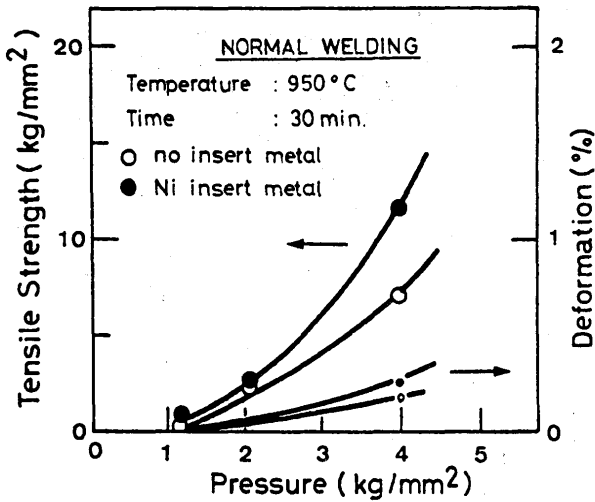


Fig. 2 Tensile strength and percent reduction in length of the weld joints obtained from one step diffusion welding as a function of the magnitude of pressure. Welding temperature and time are 950°C and 30 minutes, respectively.

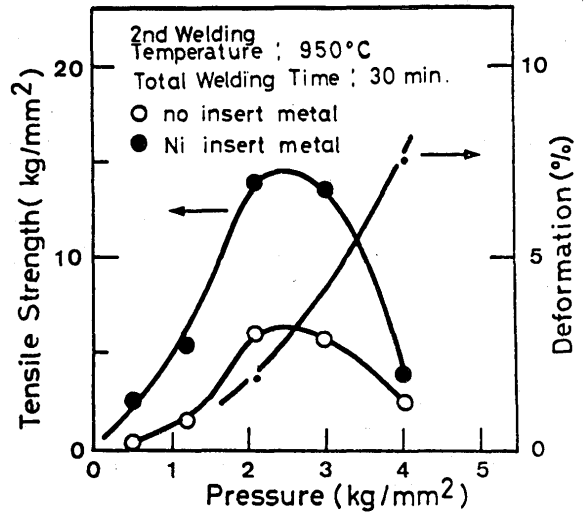


Fig. 3 Tensile strength and percent reduction in length of the weld joints obtained from the two steps diffusion welding as a function of the magnitude of pressure. For the first step welding, the temperature and time are 1200°C and 1 minute, respectively. Second step welding was performed for 29 minutes at 950°C.

strength at elevated temperatures. However, 1200°C is a maximum temperature for Hastelloy alloy X not to deform largely during 1 minute welding. For molybdenum the brittleness combined with its recrystallization behavior occurred at above 1150°C. From above discussion, the short time treatment at high welding temperature may be good among these materials in order to enhance the true metal-contact area. In this experiment, the specimens were welded by 1 minute heating at 1200°C for a initial step welding and subsequently heated for 29 minutes at various temperatures. Externally applied pressures were always 2.1 kg/mm<sup>2</sup>. Temperature of 1200°C for Hastelloy alloy X is the highest one as possible in experiment and the pressure of 2.1 kg/mm<sup>2</sup> could be adopted from the following experimental results. Figure 3 shows the tensile strength and the percent reduction in length as a function of the applied pressure. First step diffusion welding temperature,  $T_1$ , was 1200°C and the second welding temperature,  $T_0$ , was 950°C. Figure 3 shows that the magnitude of the tensile strength obtained from two steps diffusion welding under the pressure of 2.1 kg/mm<sup>2</sup> is nearly equal and/or larger, notwithstanding the existence of Ni insert-metal, than that of normal welding under the pressure of 4 kg/mm<sup>2</sup>. Percent reduction in length induced by the welding procedure become to be remarkably large and the tensile strength of weld joints become also to be lower, when the applied pressure exceeds about 2.5 kg/mm<sup>2</sup>. It is not yet clear why the magnitude of tensile strength decreased at large applied pressure.

Reasonable explanations may be concerned about formation and growth of intermetallic compounds in welding interface and also about the brittleness in molybdenum. However, the tensile strength obtained from two steps diffusion welding is clearly large under lower applied pressure comparing with the results from normal diffusion welding procedure, as shown in Fig. 3. Figure 3 indicates that the most suitable magnitude of applied pressure is about 2 kg/mm<sup>2</sup>. In Fig. 4, the both results were shown for the weld joints

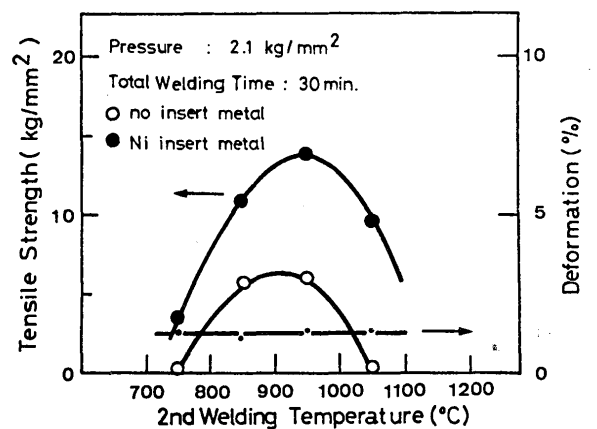
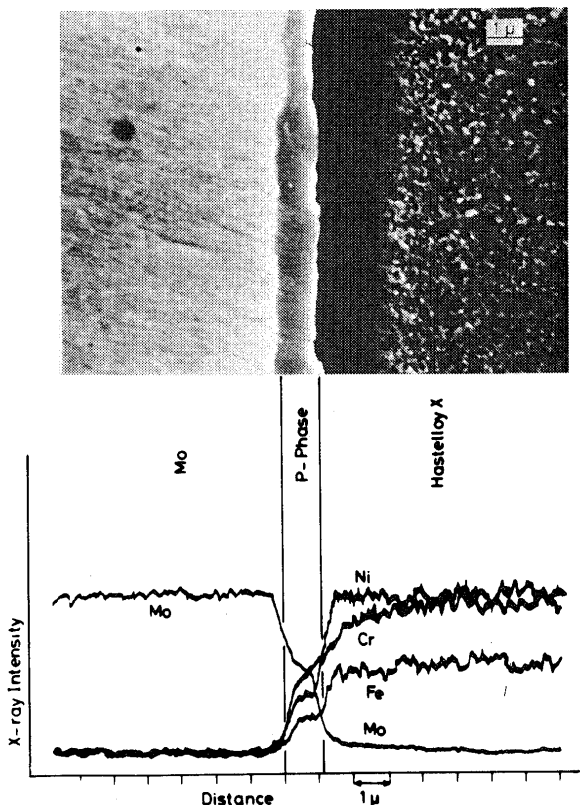


Fig. 4 Tensile strength and percent reduction in length of the weld joints as a function of the second welding temperatures. First step welding was performed for 1 minute at 1200°C under the pressure of 2.1 kg/mm<sup>2</sup>. Deformation as a percent reduction in length does not depend on the existence of Ni insert-metal.

including and without Ni insert-metal. The magnitude of percent reduction in length indicates relatively small and constant value, depending on the second diffusion welding temperature which is in the range of 750°C and 1050°C. The maximum value of tensile strength was obtained from the joint welded at 950°C of second heating temperature and that becomes to be lower when the temperature exceeds 950°C. This fact agrees fairly with the results reported previously by Hashimoto and Tanuma<sup>5)</sup> in normal diffusion welding of molybdenum plates. These tendency were found in both results from the weld joints with and without Ni insert-metal, and a use of the Ni insert-metal increases the tensile strength of the weld joint compared with the joint without Ni insert-metal.

### 3.2. Microstructure near the weld bond region and effects of Ni insert-metal.

Microscopic observations near the weld bond region using a scanning electron microscopy (SEM) were performed for the specimen whose welding conditions are as follows; second heating temperature is 950°C,



**Fig. 5** Scanning electron micrograph and the distribution of Mo, Ni, Cr and Fe near the weld bond region. Weld joint was obtained from two steps welding procedure. First step welding was performed by 1 minute annealing at 1200°C under the pressure of 2.1 kg/mm<sup>2</sup>. Second step welding was performed by 29 minutes annealing at 950°C under the same pressure.

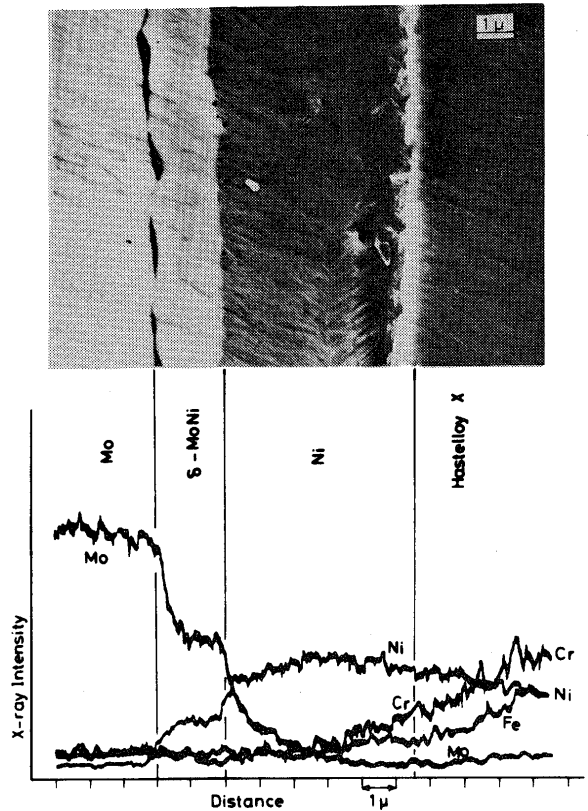


**Fig. 6** Scanning electron micrograph and the distribution of Mo, Ni, Cr and Fe near the weld bond region including Ni insert-metal. Welding procedure was completely same as in Fig. 5.

pressure 2.1 kg/mm<sup>2</sup> and total welding time 30 minutes. **Figure 5** and **6** show the scanning electron micrographs near the weld bond region and the distribution of elements as Mo, Ni, Fe and Cr all of which were analysed by SSD. Figure 5 shows the microstructure without Ni insert-metal and Fig. 6 shows that of including Ni insert-metal. From the distribution curves of the elements, it was found that the intermetallic compound containing Mo, Ni, Cr and Fe exists at weld bond region without Ni insert-metal and the binary intermetallic compound of Mo and Ni was found at weld bond with Ni insert-metal. In order to clarify these intermetallic compounds, the X-ray diffraction analysis was performed using the fractured surfaces obtained after tensile strength tests, and the results obtained are shown in **Fig. 7** and **8**. Using a fractured surface without Ni insert-metal, the obvious patterns from molybdenum and intermetallic compound, P phase<sup>6)</sup>, were obtained at the Hastelloy alloy X side and pattern from Hastelloy alloy X was not observed at molybdenum side. At molybdenum side, the patterns only from molybdenum and P phase were found out. Using a fractured surface including

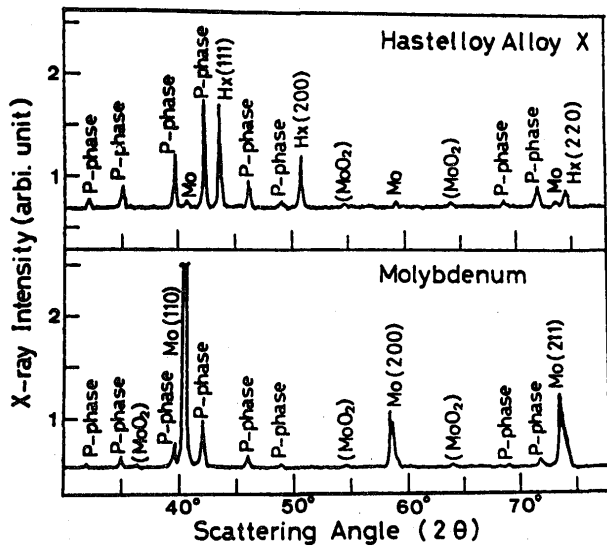


Fig. 7 X-ray diffraction patterns obtained from the fractured surfaces of weld joints. Fractured surfaces were obtained after the tensile strength test and Cu  $K_{\alpha}$  X-ray was used. Hx indicates the Hastelloy alloy X. Weld joint was obtained from the two steps welding. First step welding was performed by 1 minute annealing at 1200°C under the pressure of 2.1 kg/mm<sup>2</sup>. Second step welding was performed by 29 minutes annealing at 950°C under the same pressure.

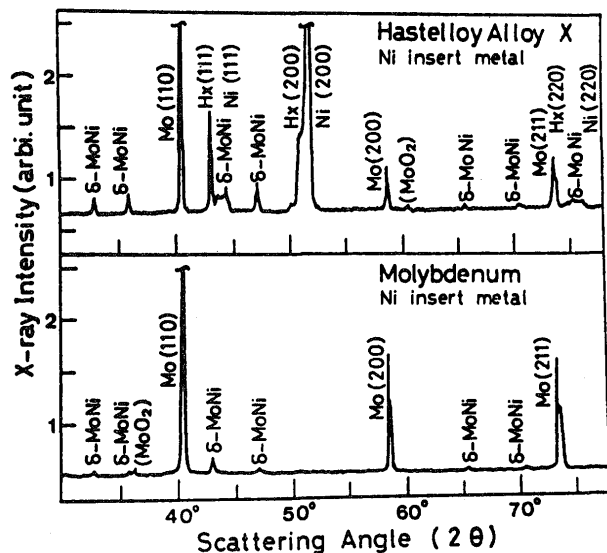


Fig. 8 X-ray diffraction patterns obtained from fractured surfaces of weld joints including Ni insert-metal. Hx indicates the Hastelloy alloy X. Specimen preparation was completely same as in Fig. 7.

Ni insert-metal, the patterns from  $\delta$ -MoNi<sup>7)</sup>, Mo, Hastelloy alloy X and Ni were obtained at the Hastelloy alloy X side, but the patterns only from Mo and  $\delta$ -MoNi were observed at molybdenum side and the lines arising from Ni and Hastelloy alloy X did not exist. Very weak diffraction pattern due to MoO<sub>2</sub> was observed from either of the fractured surfaces of weld

joints with and without Ni insert-metal. It is not clear which is true that the molybdenum oxide, MoO<sub>2</sub>, was formed during the welding procedure or during the period in keeping at ambient atmosphere after the tensile strength tests. In consequence of these X-ray diffraction analysis, it was found that the Ni insert-metal suppresses the formation of P phase, but forms the binary intermetallic compound,  $\delta$ -MoNi. Crystal structure of P phase has not yet been established, but this phase may be quite brittle like as  $\sigma$  phase appeared in Fe-Cr binary system<sup>9)</sup>. On the other words, the Ni insert-metal suppresses the formation of brittle intermetallic compound and then contributes the increase in tensile strength.

### 3.3. Fractured surface at weld joints.

As mentioned in previous section, the maximum tensile strength was obtained from the joint which was welded using two steps diffusion welding technique having a second heating temperature of 950°C and a use of the Ni insert-metal. However the value of the maximum tensile strength was still lower than that of the Mo base metal. Microscopic observations using a scanning electron microscopy (SEM) were performed in order to understand the details about the path of fracture and the conditions of fractured surface.

Photograph 1 indicates a typical scanning electron micrograph obtained from the fractured surface of molybdenum side. Grain size of the intermetallic compound,  $\delta$ -MoNi, is smaller than that of the molybdenum and the fracture occurred through the path within the  $\delta$ -MoNi compound and along the grain boundaries in molybdenum. Similar observations performed simultaneously for the surface of Hastelloy

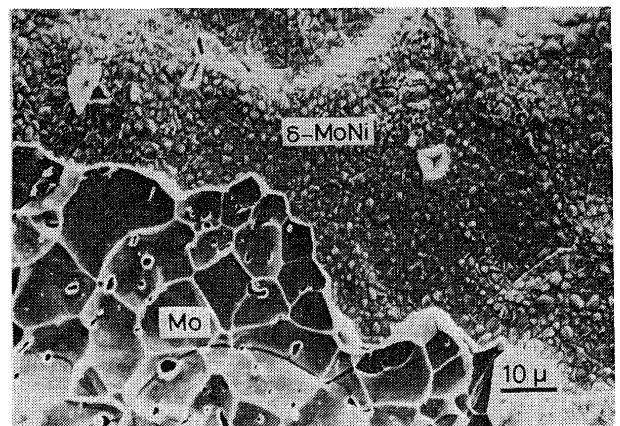
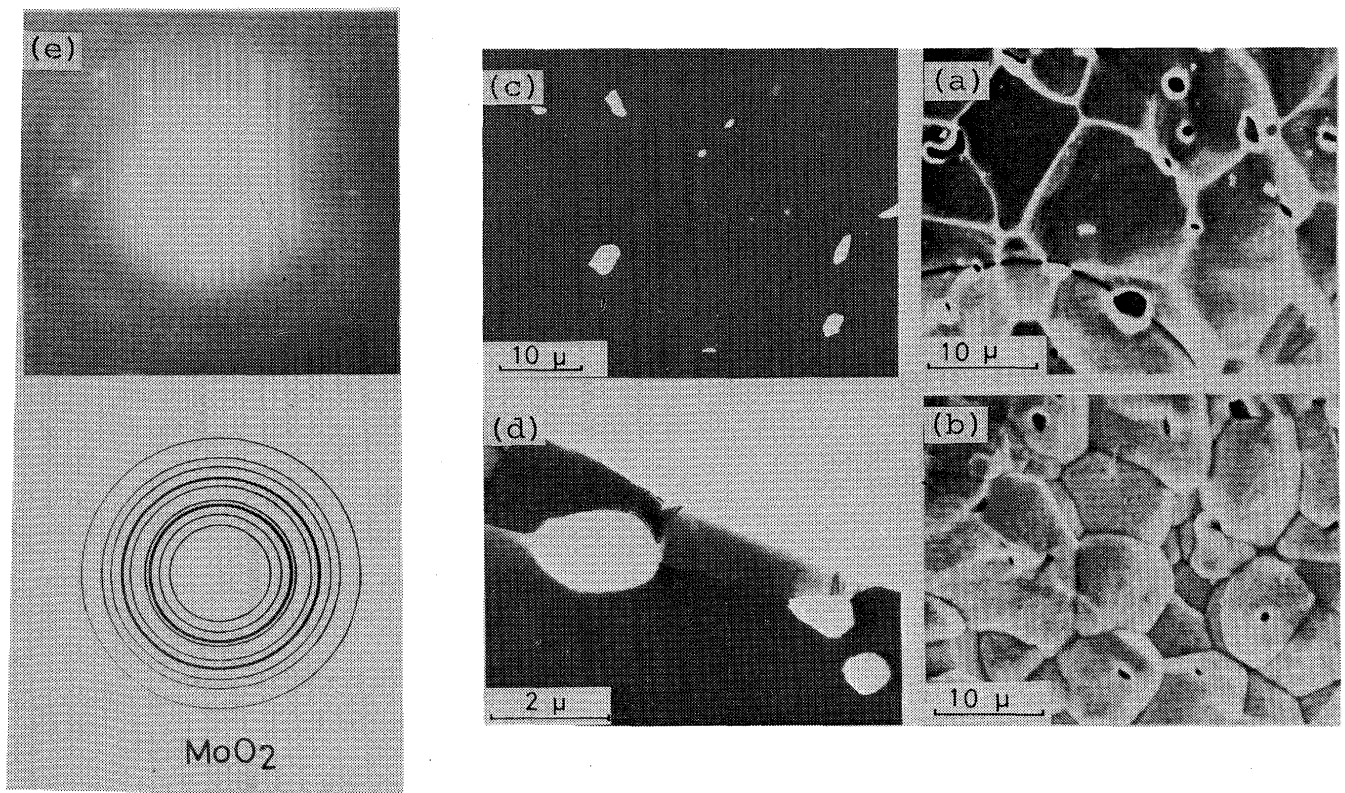


Photo. 1 Typical scanning electron micrograph obtained from the fractured surface of weld joint including Ni insert-metal. Photograph shows the molybdenum side of the weld joint.

alloy X and showed the fracture had occurred surely like as mentioned above. These results agree well with the results from X-ray diffraction analysis as shown in Fig. 8. X-ray diffraction analysis indicated that the molybdenum side in fractured surface consists of Mo and  $\delta$ -MoNi, but there are Mo,  $\delta$ -MoNi, Ni and Hastelloy alloy X in the side of Hastelloy alloy X. For the weld joints without Ni insert-metal, the fracture occurred through the path within P phase and Mo, like as deduced in Fig. 7. Many number of voids which have various size around a few micron in diameter were observed along the grain boundaries in molybdenum of Photo. 1. Microscopic observation using a transmission electron microscopy (TEM) for thin foil specimens of molybdenum which were cut from the region apart 1 mm from the fractured interface, in order to judge that these voids exist only near the bond region or in everywhere of molybdenum.

**Photograph 2** indicates the typical transmission electron micrograph as in (c) and (d) obtained from molybdenum apart 1 mm from the bond region and the scanning electron micrograph as in (a) and (b) obtained from the fractured surface of molybdenum. There are many voids in transmission electron micrograph which have size of a few micron in diameter and identical with those observed in scanning electron micrograph. (e) in Photo. 2 shows the selected area diffraction pattern obtained from the region near the voids. Diffraction pattern seems to be identical with the schematic drawing down below the photograph, which is the ring pattern for polycrystalline  $\text{MoO}_2$ . From above facts, it was found that the many numbers of voids exist along the grain boundaries in molybdenum after the welding procedure and also exist the oxide,  $\text{MoO}_2$ , in the region around some voids. It is said that, for vacuum condition, an oxidized molyb-



**Photo. 2** Microstructure of molybdenum in the weld joint. Scanning electron micrographs (a) and (b) show the fractured molybdenum surfaces. (a) molybdenum side. (b) Hastelloy alloy X side. Transmission electron micrograph (c) and (d) were obtained from thin foil molybdenum base metal which was cut from inner region of about 1 mm apart from fractured molybdenum surface. Selected area diffraction pattern (e) was obtained from the region around the void.

denum sample will lose  $\text{MoO}_3$ , leaving  $\text{MoO}_2$  solid on the surface<sup>9)</sup>. The origin of the formation of the voids may be considered as a result from evaporation and/or volatilization of these oxides, but detailed behaviors at grain boundaries in molybdenum are not yet clear about these oxides. Consequently the existence of these voids affected harmfully for the tensile strength of weld joints, since the fracture had occurred through the path along the grain boundaries of molybdenum base metal.

#### 4. Conclusive Remarks.

In this investigation, the diffusion welding between pure molybdenum and heat-resisting alloy Hastelloy X has been performed in vacuum, as typical application of the diffusion bonding in dissimilar materials for which it is quite difficult to get the good weld joints by usual methods in fusion welding techniques. Application of two steps diffusion welding technique and a use of the Ni insert-metal are discussed in terms of the tensile strength of weld joints from room temperature measurements. Brittleness in molybdenum also discussed by microscopic observations using SEM and TEM techniques.

Results obtained are summarized as follows;

- (1) Two steps welding technique including short time heating at high temperature (1 minute at  $1200^\circ\text{C}$ ) increases the real metal-contact between molybdenum and Hastelloy alloy X and takes the improvements of the joint strength. Furthermore, this technique is useful not to enlarge the deformation by welding procedure.
- (2) Application of the Ni insert-metal suppresses the formation of the brittle intermetallic compound, P

phase, and increases the joint strength. However, the formation of binary intermetallic compound,  $\delta\text{-MoNi}$  was observed at the bonding interface.

- (3) Fracture in weld joints induced by tensile strength tests had occurred always through the intermetallic compounds and also along the grain boundaries of molybdenum base metal.
- (4) After the welding procedure, the voids and molybdenum oxide,  $\text{MoO}_2$ , were found out at the grain boundaries in molybdenum using SEM and TEM techniques.

#### Acknowledgments

Many thanks are due to Mr. T. Horinouchi for his help throughout this work.

#### References

- 1) Summary Report of Japan Atomic Energy Research Institute of Tokai Establishment; Current Status in the Development of Fusion Reactor, (1975), (in Japanese).
- 2) N. F. Kazakov; Diffusionaya Svarka Vakuume, Mashinostroyeniye, (1968).
- 3) T. Enjyo, K. Ikeuchi, T. Iida, M. Kanai and Y. Arata; Diffusion Welding of Ti-15%Mo-5%Zr Alloy to Mild Steel (0.06%C), J. High Temp. Soc., 2-1 (1976) 36, (in Japanese).
- 4) T. Enjyo, K. Ikeuchi, M. Kanai and T. Maruyama; Diffusion Welding of Titanium to Aluminum, J. Japan Weld. Soc., 46-2 (1977) 32, (in Japanese).
- 5) T. Hashimoto and K. Tanuma; Diffusion Welding of Molybdenum, J. Japan Weld. Soc., 37 (1968) 1345, (in Japanese).
- 6) T. Wada; Metals Handbook, 8th edition, Vol. 8, Metallography, Structures and Phase Diagram, ASM, Ohio (1973) 426.
- 7) C. B. Shoemaker and D. P. Shoemaker; The Crystal Structure of the  $\delta$ -Phase, MoNi, Acta Cryst., 16 (1963) 997.
- 8) E. A. Gulbransen and S. A. Jansson; Oxidation of Metals and Alloys, ASM, Metals Park, Ohio (1971) 75.